Multispectral terahertz sensing with highly flexible ultrathin metamaterial absorber

Yahiaoui, Riad; Tan, Siyu; Cong, Longqing; Singh, Ranjan; Yan, Fengping; Zhang, Weili

2015

Yahiaoui, R., Tan, S., Cong, L., Singh, R., Yan, F., & Zhang, W. (2015). Multispectral terahertz sensing with highly flexible ultrathin metamaterial absorber. Journal of Applied Physics, 118(8), 083103-.

https://hdl.handle.net/10356/79325

https://doi.org/10.1063/1.4929449

Multispectral terahertz sensing with highly flexible ultrathin metamaterial absorber

Riad Yahiaoui, Siyu Tan, Longqing Cong, Ranjan Singh, Fengping Yan, and Weili Zhang

Citation: Journal of Applied Physics **118**, 083103 (2015); doi: 10.1063/1.4929449
View online: http://dx.doi.org/10.1063/1.4929449
View Table of Contents: http://scitation.aip.org/content/aip/journal/jap/118/8?ver=pdfcov
Published by the AIP Publishing

JOURNAL OF APPLIED PHYSICS **118**, 083103 (2015)

Multispectral terahertz sensing with highly flexible ultrathin metamaterial absorber

Riad Yahiaoui,[1,a)] Siyu Tan,[2,3] Longqing Cong,[4,5] Ranjan Singh,[4,5,a)] Fengping Yan,[3] and Weili Zhang[2]
[1]*XLIM, Limoges University, CNRS, UMR 7252, 7 rue Jules Vallès, F-19100 Brive, France*
[2]*School of Electrical and Computer Engineering, Oklahoma State University, Stillwater, Oklahoma 74078, USA*
[3]*Key Lab of All Optical Network and Advanced Telecommunication Network of EMC, Institute of Lightwave Technology, Beijing Jiaotong University, Beijing 100044, People's Republic of China*
[4]*Division of Physics and Applied Physics, School of Physical and Mathematical Sciences, Nanyang Technological University, Singapore 637371, Singapore*
[5]*Centre for Disruptive Photonic Technologies, School of Physical and Mathematical Sciences, Nanyang Technological University, Singapore 637371, Singapore*

(Received 2 May 2015; accepted 11 August 2015; published online 26 August 2015)

We report the simulation, fabrication, and experimental characterization of a multichannel metamaterial absorber with the aim to be used as a label-free sensing platform in the terahertz regime. The topology of the investigated resonators deposited on a thin flexible polymer by means of optical lithography is capable of supporting multiple resonances over a broad frequency range due to the individual contribution of each sub-element of the unit cell. In order to explore the performance of the chosen structure in terms of sensing phenomenon, the reflection feature is monitored upon variation of the refractive index and the thickness of the analyte. We achieve numerically maximum frequency sensitivity of about 139.2 GHz/refractive index unit. Measurements carried out using terahertz time-domain spectroscopy show good agreement with the numerical predictions. The results are very promising, suggesting a potential use of the metamaterial absorber in wide variety of multispectral terahertz sensing applications. © *2015 AIP Publishing LLC*.
[http://dx.doi.org/10.1063/1.4929449]

I. INTRODUCTION

In recent years, there has been a renewed interest in the property of near perfect absorption (NPA) from the scientific community, originally used in stealth technology to reduce radar cross section (RCS) of objects at specific radar frequencies. The advent of metamaterials (MMs) with unique properties played a key role in the development of high quality absorbers ranging from microwaves to optical wavelengths[1–12] and their integration in numerous functional applications such as imaging[13,14] and solar energy collection.[15,16] The terahertz (THz) regime, which extends from 100 GHz to 10 THz, is a particularly interesting region that has remained inaccessible for a long time due to the unavailability of appropriate emitters and detectors.

In the past two decades, the field of terahertz technology has experienced remarkable development due to advances in laser and semiconductor technology. This has given rise to various potential applications including subdiffraction imaging,[17] cloaking,[18] and polarization conversion systems.[19,20] Sensing applications have also a strong potential to benefit from terahertz technology, which provides unprecedented probing capabilities. Fluorescent labeling is the most common technique for tracking and monitoring biomolecules such as proteins, antibodies, or amino acids. However, attaching a chemically fluorescent substance to unknown molecules is a very expensive and complicated process. Furthermore, this treatment may considerably modify the sample and significantly lower the precision of the diagnostic due to certain drawbacks.[21] Therefore, it is more desirable to develop novel label-free detection approaches, which should be simultaneously highly sensitive and selective, possibly biocompatible, and immune to external disturbances such as pressure or temperature changes. The sensing capability in the terahertz regime is enhanced by the exceptional behaviors of metamaterials. Various studies have explored the use of metamaterials as label-free low-cost, compact and high-performing biosensors, thereby offering an alternative approach to detect and identify small chemical and biomolecular compounds.[21–31] Among the myriad applications of metamaterials, perfect metamaterial absorbers (PMAs) have emerged as potential candidates for absorbing electromagnetic waves.[1–12] The basic approach is to minimize the reflection from the metamaterial absorber (MA) by matching the impedance to free space and simultaneously suppress the transmission by using a metallic ground plane layer. As a consequence, excitation light could be locally stored inside the structure for a finite time, thus enhancing the interaction with an attached analyte dramatically, which constitutes therefore an attractive concept for bio-sensing applications. Additionally, the ground plane isolates the interaction between the metamaterial device and the substrate, eliminating the detrimental effect of electric field decay in typically high dielectric substrates. We exploit these two distinct

[a)]Authors to whom correspondence should be addressed. Electronic addresses: riad.yahiaoui@unilim.fr and ranjans@ntu.edu.sg

features of PMAs for enhanced light matter interaction and demonstrate a multispectral metamaterial absorber with enhanced sensing capabilities in the terahertz spectral range.

II. PRESENTATION OF THE MULTISPECTRAL METAMATERIAL ABSORBER

Our proposed multispectral THz metamaterial absorber consists of two metallic layers separated by a dielectric spacer. The top layer consists of an array of planar metallic resonators (made of 200 nm thick aluminum) that combines an inner cut wire (CW) and an outer two-gap split ring resonator (SRR). They have been deposited periodically on the top side of 50 μm thick dielectric spacer (commercially available Kapton® polyimide film with a dielectric constant of $\varepsilon_r = 3 + 0.15i$) using a lithography-based patterning process and are responsible for determining the absorption frequencies. The bottom side of the dielectric spacer is entirely coated with 200 nm thick aluminum, acting as a ground plane to inhibit any transmission through the structure.

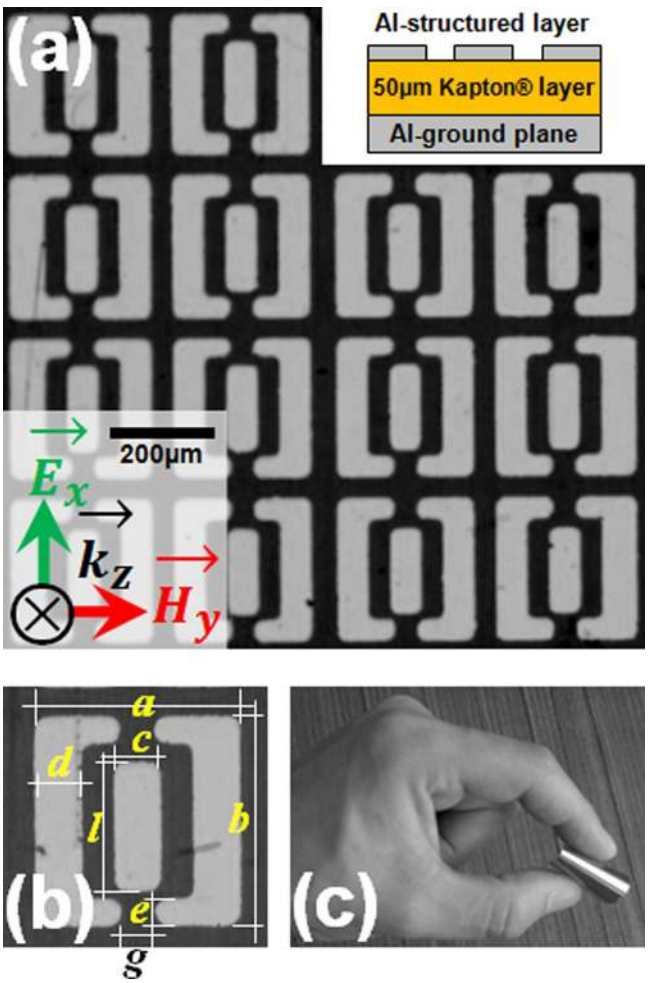

FIG. 1. (a) Scanning electron microscope (SEM) image of the fabricated metamaterial absorber with a schematic cross-section of the sample (top right) and the polarization of the incident plane wave (bottom left). (b) Representation of a single unit cell with the relevant geometrical dimensions: $a = b = 250\,\mu$m, $c = d = g = 50\,\mu$m, $e = 25\,\mu$m, and $l = 155\,\mu$m. The unit cells are arranged in the periods of $p_x = p_y = 300\,\mu$m. (c) The fabricated metamaterial absorber is caught between two fingers to illustrate its large flexibility.

Figure 1(a) represents the scanning electron microscope (SEM) image of the fabricated MA, a schematic of its cross-section (top right) and the polarization of the incident plane wave (bottom left). The single unit cell of the fabricated MA is represented in Fig. 1(b) with the relevant geometrical dimensions: $a = b = 250\,\mu$m, $c = d = g = 50\,\mu$m, $e = 25\,\mu$m $l = 155\,\mu$m. The unit cells are arranged in the periods of $p_x = p_y = 300\,\mu$m. Originally, the design of the metasurface (i.e., SRR and CW without the metallic ground plane) was introduced in earlier work to investigate some specific coupling effects between the SRR and the CW.[32] In this paper, we have reconsidered the structure as a multiband MA for a potential use in sensing applications. The multilayer topology (i.e., metal–dielectric–metal triple layer) of a MA can be assimilated to a Fabry-Pérot (FP) resonant cavity that absorbs light due to constructive interference between multiple reflections that occur between the structured layer (i.e., the metasurface) and the metallic ground plane.[33–35] Basically, the metasurface determines the absorption frequency, the metallic back layer reflects the transmitted resonance frequency, and the spacer layer acts as a subwavelength cavity, which makes the waves reflected from the metallic layer out of phase with respect to the reflected waves from the metasurface.[36] Such a cavity scheme has been widely used to demonstrate subwavelength highly directive antennas at microwave frequencies.[37–41] Due to the highly flexible and ultrathin nature of the absorber, the chosen sensor design is very appropriate for non-planar applications [see Fig. 1(c)]. Recently, there have been various efforts devoted to realize flexible metamaterials.[9,32,42–48] The use of flexible substrates has provided an unprecedented route to achieve frequency tunable metamaterials due to modifications in the profiles and the periodicities of the structures when the substrates are stretched.[49–54]

III. ANALYSIS OF THE ELECTROMAGNETIC RESPONSE OF THE METAMATERIAL ABSORBER

We studied the electromagnetic behavior of the structure using a finite element method (FEM). In these calculations, the elementary cell of the designed metamaterial was irradiated by a normally incident plane wave with the electric field parallel to the x-axis and the magnetic field parallel to the y-axis. Periodic boundary conditions were applied in the numerical model in order to mimic a 2D infinite structure. In the simulations, the aluminum was modelled as a lossy metal with a conductivity of $\sigma_{Al} = 3.45 \times 10^7$ S/m. The active surface of the fabricated device is about 2 cm × 2 cm square. Measurements using terahertz time-domain spectroscopy (THz–TDS) in reflection configuration and under normal incidence were carried out in dry-air environment in order to determine the response of the structure to an incident terahertz electromagnetic wave.[55,56] The THz–TDS system was comprised of a GaAs photoconductive transmitter and a silicon-on-sapphire (SOS) photoconductive receiver, each was optically excited with 26-fs ultrafast optical pulses of 10 mW average power. The THz–TDS system was configured in an 8F confocal geometry and a 3.5-mm frequency-independent beam waist. The amplitude of the reflection is

defined as $|r(\omega)| = |E_{sr}(\omega)/E_i(\omega)|$, where $E_{sr}(\omega)$ is the measured reflection spectrum. It is normalized by $E_i(\omega)$ with respect to the reflection amplitude of an aluminum coated silicon wafer.[57] In our measurements, 512 data points were sampled to form a time domain pulse through adjusting the time delay line between each sampling process. The additional length of time-delay line is 10 μm. Therefore, the total duration of the time-domain pulse can then be calculated as $T = 512 \times (10\,\mu\text{m}/c) \approx 17$ ps, where c is the speed of light. After the Fourier transformation, the corresponding frequency resolution of the setup is $1/T \approx 58.8$ GHz. The simulated (solid line) and measured (dashed line) reflection and absorption spectra of the metamaterial absorber are plotted in Fig. 2(a) and reveal mainly three resonant modes. The structure supports multiple resonances at around 0.22 THz, 0.48 THz, and 0.76 THz, respectively. Although there are minor differences in amplitude and bandwidth of the resonances (probably due to some imperfections during the manufacturing process), the spectra obtained from measurements confirm very well the trends predicted by numerical calculations. To deepen in the origin of the resonances, the magnetic field amplitude distributions for the metamaterial absorber were simulated and plotted in Figs. 2(b)–2(e) at absorption frequencies of 0.22 THz, 0.48 THz, 0.72 THz, and 0.76 THz, respectively, at $z = 0$ cut-plane. The lowest resonance at around 0.22 THz stems from the excitation of the SRR. The magnetic field expands along every arm of the SRR [Fig. 2(b)] and gives rise to a dipole resonant frequency. At the resonant frequency of 0.48 THz, we observe strong magnetic field localization along the CW [Fig. 2(c)]. The third resonance splits into two distinct resonances at around 0.72 THz and 0.76 THz, respectively. The geometry and the dimensions of the structure have not been specifically chosen to create the splitting around the third resonance. We have performed further numerical calculations (but not shown here), which confirm that when the two resonators (i.e., SRR and CW) are brought closer in space (i.e., embedded into one single elementary cell), they mutually couple to one another, thus altering their resonant response in a behavior commonly known as hybridization or resonant splitting. The coupling between the resonators is weak [see Figs. 2(d)–2(e)]. This reduces the hybridization effects and the two resonances occur very close to each other.[58]

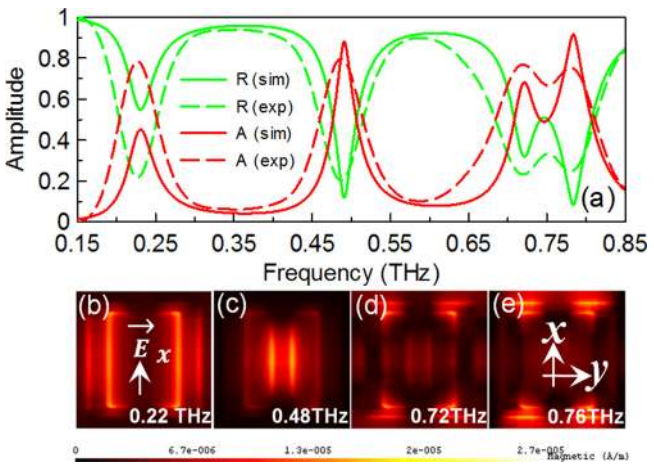

FIG. 2. (a) Simulated (solid line) and measured (dashed line) reflection R and absorption A spectra of the metamaterial absorber. (b)–(e) Simulated spatial distribution of the resonant magnetic field H for a single unit cell of the metamaterial absorber illuminated by a plane wave, at absorption frequencies of 0.22 THz, 0.48 THz, 0.72 THz, and 0.76 THz, respectively, at $z = 0$ cut-plane.

IV. EVALUATION OF THE SENSING PERFORMANCE OF THE MULTISPECTRAL METAMATERIAL ABSORBER

The sensing mechanism reported in this work is mainly based on modifications in the optical thickness of the surrounding medium of the metamaterial absorber (i.e., the refractive index n and the thickness of the analyte embedded in the structure, which are inherent parameters in organic systems). The sensing device is now fully coated (on top of CWs and SRRs) by an overlayer with a thickness of 50 μm, a dielectric constant of 3 (i.e., $n_{\text{analyte}} = 1.73$), and a loss tangent of 0.05. The test sample (analyte) is chosen in such a way that its refractive index ($n_{\text{analyte}} = 1.73$) is comparable to some real bio-materials). For example, it is worth noting that the refractive index of biomolecules can vary from 1.4 to 1.6 in DNA and in the range between 1.6 and 2.0 in RNA.[59,60] The simulated and measured amplitude reflection spectra without analyte and with 50-μm-thick analyte ($n_{analyte} = 1.73$) are plotted in Figs. 3(a) and 3(b), respectively. When the refractive index is increased, the resonances shift to lower frequencies due to the increase in the optical thickness of the structure along the direction of wave propagation k. In other words, the reason of this shift can be explained by the change in capacitance of the structure. Upon loading with small amount of dielectric material, the capacitance value increases and the resonances shift towards lower frequencies. This red shift is noticeably accompanied by a modulation of the amplitudes of the resonances as the refractive index of the overlayer increases. In order to quantify the performance of the sensor in terms of sensing capabilities, the refractive index of the analyte is changed numerically in the range 1–2. The frequency shift (Δf) that is directly related with the sensitivity of the sensor is shown as a

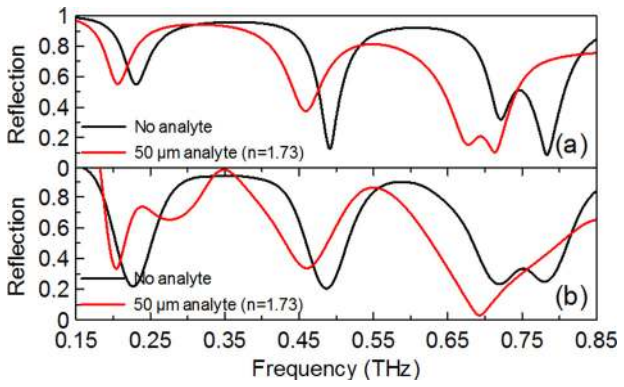

FIG. 3. (a) Simulated reflection spectra of the metamaterial absorber versus frequency without analyte and with 50-μm-thick analyte ($n_{analyte} = 1.73$). (b) The corresponding measured reflection spectra.

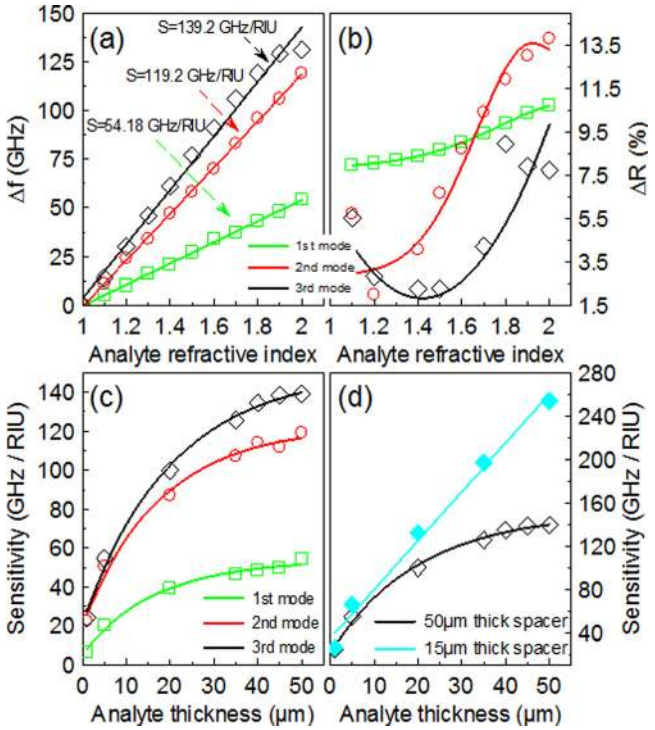

FIG. 4. (a) Frequency shift (Δf) and (b) amplitude modulation (ΔR) versus analyte refractive index for the different resonant modes of the metamaterial absorber-based sensor device. (c) Frequency sensitivity (FS) of the resonant modes as a function of the analyte thickness. (d) Frequency sensitivity of the third resonant mode as a function of the analyte thickness at dielectric spacer thicknesses of 50 μm and 15 μm, respectively. The symbols represent the exact values, while the solid lines are the fitting functions.

function of the refractive index of the analyte in Fig. 4(a). The frequency shift of the resonances (appearing nominally at $f_{R1} = 0.22$ THz, $f_{R2} = 0.48$ THz, and $f_{R3} = 0.76$ THz, respectively) increases linearly with the increase of the refractive index of the analyte. Linear fitting functions were used in order to fit the curves and to evaluate the frequency sensitivity (FS) of the sensor. The fitting functions are described by $\Delta f_{mode1} = 54.18 \times n_{analyte} - 54.45$, $\Delta f_{mode2} = 119.2 \times n_{analyte} - 120$, and $\Delta f_{mode3} = 139.2 \times n_{analyte} - 135.8$. The frequency shift ($\Delta f$) reaches a moderate value of about 54 GHz for the first resonant mode, 119 GHz for the second resonant mode, and 131 GHz for the third resonant mode at $n = 2$, which yields sensitivities (defined as the slope of the linear fitting functions $S = df/dn$, where df represents the change in the resonance frequency and dn represents the change in the refractive index) of about 54.18 GHz/refractive index unit (RIU), 119.2 GHz/RIU, and 139.2 GHz/RIU, respectively [Fig. 4(a)]. The amplitude modulation of the reflectivity (ΔR) is also investigated through numerical calculations, as shown in Fig. 4(b). Upon increasing the refractive index of the analyte and depending on the excited resonant mode, their amplitude variation as a function of the refractive index could be very different with a common nonlinear evolution. The amplitude of the first resonant mode ($f_{R1} = 0.22$ THz) presents a hyperbolic increase as a function of the terahertz refractive index of the overlayer. The amplitude of the second resonant mode ($f_{R2} = 0.48$ THz) increases exponentially and reaches a saturation beyond a refractive index of about $n = 2$. The amplitude modulation of the third resonant mode ($f_{R3} = 0.76$ THz) passes by a minimum around $n = 1.4$ and then continues to grow for reaching an amplitude modulation of about 10% at $n = 2$.

We further investigated the impact of the analyte thickness ($t_{analyte}$) on the characteristic of the sensor through detailed simulations. The metamaterial absorber is loaded by a thin film layer with dielectric properties ($\varepsilon_r = 3$ and tan $\delta = 5\%$, which corresponds to a refractive index of about $n = 1.73$). The thickness of the overlayer is changed numerically in the range 1–50 μm in order to evaluate the frequency sensitivity of the sensor as a function of the analyte thickness. Upon increasing the analyte thickness, a similar red shift of the resonances is observed. Based on the frequency shift with the change in analyte thicknesses, we estimated the frequency sensitivity of the sensor, as it is depicted in Fig. 4(c). One can observe that the FSs of the resonances follow exponential evolutions described by $FS_{mode1} = 54 - 46 \times \exp[-0.06 \times (t_{analyte} - 1)]$, $FS_{mode2} = 122 - 97 \times \exp[-0.057 \times (t_{analyte} - 1)]$, and $FS_{mode3} = 151 - 123 \times \exp[-0.049 \times (t_{analyte} - 1)]$. We also notice that the third resonant mode is more sensitive than the first and the second resonance, since it induces significantly larger frequency sensitivity and eventually reaches almost 140 GHz/RIU for an overlayer thickness of 50 μm, which is higher than the values reported in the THz regime.[61–65] We performed further simulations in order to evaluate the effect of the dielectric spacer on the characteristic of the sensor. We reduced the thickness of the dielectric substrate to 15 μm, and then we calculated the frequency sensitivity versus analyte thickness. The result of our investigations is reported in Fig. 4(d) for the third resonant mode of the metamaterial absorber. The non-linearity of the variation is weak such that a linear approximation is possible over the whole range of values of the analyte thickness. The frequency sensitivity of the third resonant mode in the case of 50 μm thick dielectric spacer is also represented for comparison. One can analyze the data in two analyte thickness regions. When the thickness of the overlayer is less than 20 μm, the sensitivity of the sensor is not dramatically enhanced as compared to the nominal case (i.e., 50-μm-thick spacer) [see Fig. 4(d)]. By contrast, the terahertz sensor becomes extremely sensitive and shows much larger sensitivity values if the thickness of the analyte is larger than 20 μm. For an intermediate value of the analyte thickness of 25 μm, the frequency sensitivity increases from 108 GHz/RIU to 153 GHz/RIU when the substrate thickness decreases from 50 μm to 15 μm [see Fig. 4(d)]. The intrinsic topology of the metamaterial absorber (dielectric spacer and the geometry of the resonators) makes the sensor highly sensitive, and the frequency sensitivity could be further enhanced by investigating different architectures of the resonators.

V. CONCLUSION

In summary, we have designed, fabricated, and experimentally characterized a multiband ultrathin and highly flexible metamaterial absorber that was used for sensing application in the terahertz regime. The proposed sensing

device showed extremely high sensitivities in the presence of small amount of the substance to be analyzed. The compactness of the entire structure, the simple topology of the resonators, and the use of a dielectric substrate with high mechanical flexibility are all key parameters suggesting a possible integration scheme of terahertz biosensors on-chip. This is a very promising step towards mass production of low cost and easily manufacturable novel terahertz sensing devices inspired from the technology of metamaterials.

ACKNOWLEDGMENTS

This work was initiated at XLIM, Limoges University. Ranjan Singh would like to thank his start up Grant No. M4081282.

[1]X. Shen, T. J. Cui, J. Zhao, H. F. Ma, W. X. Jiang, and H. Li, Opt. Express **19**, 9401–9407 (2011).
[2]H. Li, L. H. Yuan, B. Zhou, X. P. Shen, Q. Cheng, and T. J. Cui, J. Appl. Phys. **110**, 014909 (2011).
[3]F. Ding, Y. Cui, X. Ge, Y. Jin, and S. He, Appl. Phys. Lett. **100**, 103506 (2012).
[4]D. Wen, H. Yang, Q. Ye, M. Li, L. Guo, and J. Zhang, Phys. Scr. **88**, 015402 (2013).
[5]H. Tao, N. I. Landy, C. M. Bingham, X. Zhang, R. D. Averitt, and W. J. Padilla, Opt. Express **16**, 7181–7188 (2008).
[6]H. Tao, C. M. Bingham, D. Pilon, K. Fan, A. C. Strikwerda, D. Shrekenhamer, W. J. Padilla, X. Zhang, and R. D. Averitt, J. Phys. D: Appl. Phys. **43**, 225102 (2010).
[7]Y. Q. Ye, Y. Jin, and S. He, J. Opt. Soc. Am. B **27**, 498–504 (2010).
[8]J. Grant, Y. Ma, S. Saha, A. Khalid, and D. R. S. Cumming, Opt. Lett. **36**, 3476–3478 (2011).
[9]R. Yahiaoui, J. P. Guillet, F. de Miollis, and P. Mounaix, Opt. Lett. **38**, 4988–4990 (2013).
[10]R. Yahiaoui, K. Hanai, K. Takano, T. Nishida, F. Miyamaru, M. Nakajima, and M. Hangyo, Opt. Lett. **40**, 3197–3200 (2015).
[11]J. A. Bossard, L. Lin, S. Yun, L. Liu, D. H. Werner, and T. S. Mayer, ACS Nano **8**, 1517–1524 (2014).
[12]Y. Z. Cheng, W. Withayachumnankul, A. Upadhyay, D. Headland, Y. Nie, R. Z. Gong, M. Bhaskaran, S. Sriram, and D. Abbott, Adv. Opt. Mater. **3**, 376–380 (2015).
[13]N. I. Landy, C. M. Bingham, T. Tyler, N. Jokerst, D. R. Smith, and W. J. Padilla, Phys. Rev. B **79**, 125104 (2009).
[14]S. A. Kuznetsov, A. G. Paulish, A. V. Gelfand, P. A. Lazorskiy, and V. N. Fedorinin, Prog. Electromagn. Res. **122**, 93–103 (2012).
[15]T. Stelzner, M. Pietsch, G. Andrä, F. Falk, E. Ose, and S. Christiansen, Nanotechnology **19**, 295203 (2008).
[16]Y. Wang, T. Sun, T. Paudel, Y. Zhang, Z. Ren, and K. Kempa, Nano Lett. **12**, 440–445 (2012).
[17]A. Tuniz, K. J. Kaltenecker, B. M. Fischer, M. Walther, S. C. Fleming, A. Argyros, and B. T. Kuhlmey, Nat. Commun. **4**, 2706 (2013).
[18]D. P. Gaillot, C. Croënne, and D. Lippens, Opt. Express **16**, 3986–3992 (2008).
[19]L. Cong, W. Cao, X. Zhang, Z. Tian, J. Gu, R. Singh, J. Han, and W. Zhang, Appl. Phys. Lett. **103**, 171107 (2013).
[20]N. K. Grady, J. E. Heyes, D. R. Chowdhury, Y. Zeng, M. T. Reiten, A. K. Azad, A. J. Taylor, D. A. R. Dalvit, and H. T. Chen, Science **340**, 1304–1307 (2013).
[21]C. Debus and P. H. Bolivar, Appl. Phys. Lett. **91**, 184102 (2007).
[22]H. Yoshida, Y. Ogawa, Y. Kawai, S. Hayashi, A. Hayashi, C. Otani, E. Kato, F. Miyamaru, and K. Kawase, Appl. Phys. Lett. **91**, 253901 (2007).
[23]J. F. O'Hara, R. Singh, I. Brener, E. Smirnova, J. Han, A. J. Taylor, and W. Zhang, Opt. Express **16**, 1786–1795 (2008).
[24]E. Cubukcu, S. Zhang, Y. S. Park, G. Bartal, and X. Zhang, Appl. Phys. Lett. **95**, 043113 (2009).
[25]H. Tao, L. R. Chieffo, M. A. Brenckle, S. M. Siebert, M. Liu, A. C. Strikwerda, K. Fan, D. L. Kaplan, X. Zhang, R. D. Averitt, and F. G. Omenetto, Adv. Mater. **23**, 3197–3201 (2011).
[26]M. D. Rotaru and J. K. Sykulski, IEEE Trans. Magn. **47**, 1026–1029 (2011).
[27]X. Wu, Y. E, X. Xu, and L. Wang, Appl. Phys. Lett. **101**, 033704 (2012).
[28]Y. Ma, H. Zhang, Y. Li, Y. Wang, and W. Lai, Prog. Electromagn. Res. **138**, 407–419 (2013).
[29]X. Wu, X. Pan, B. Quan, X. Xu, C. Gu, and L. Wang, Appl. Phys. Lett. **102**, 151109 (2013).
[30]F. Miyamaru, K. Hattori, K. Shiraga, S. Kawashima, S. Suga, T. Nishida, M. W. Takeda, and Y. Ogawa, J Infrared Milli Terahertz Waves **35**, 198–207(2014).
[31]R. Singh, W. Cao, I. Al-Naib, L. Cong, W. Withayachumnankul, and W. Zhang, Appl. Phys. Lett. **105**, 171101 (2014).
[32]R. Yahiaoui, K. Takano, F. Miyamaru, M. Hangyo, and P. Mounaix, J. Opt. **16**, 094014 (2014).
[33]H.-T. Chen, Opt. Express **20**, 7165–7172 (2012).
[34]L. Huang, D. R. Chowdhury, S. Ramani, M. T. Reiten, S.-N. Luo, A. K. Azad, A. J. Taylor, and H.-T. Chen, Appl. Phys. Lett. **101**, 101102 (2012).
[35]L. Cong, S. Tan, R. Yahiaoui, F. Yan, W. Zhang, and R. Singh, Appl. Phys. Lett. **106**, 031107 (2015).
[36]P. Kung and S. M. Kim, in *PIERS Proceedings, March 25–28, Taipei* (2013), pp. 232–235.
[37]A. P. Feresidis, G. Goussetis, S. Wang, and J. C. Vardaxoglou, IEEE Trans. Antennas Propag. **53**, 209–215 (2005).
[38]L. Zhou, H. Li, Y. Qin, Z. Wei, and C. T. Chan, Appl. Phys. Lett. **86**, 101101 (2005).
[39]R. Yahiaoui, S. N. Burokur, and A. de Lustrac, Electron. Lett. **45**, 814–816 (2009).
[40]R. Yahiaoui, S. N. Burokur, V. Vigneras, A. de Lustrac, and P. Mounaix, Microwave Opt. Technol. Lett. **54**, 1327–1332 (2012).
[41]R. Yahiaoui, R. Chantalat, N. Chevalier, M. Jouvet, and M. Lalande, Prog. Electromagn. Res. C **44**, 185–195 (2013).
[42]I. M. Pryce, K. Aydin, Y. A. Kelaita, R. M. Briggs, and H. A. Atwater, Nano Lett. **10**, 4222–4227 (2010).
[43]P. K. Singh, K. A. Korolev, M. N. Afsar, and S. Sonkusale, Appl. Phys. Lett. **99**, 264101 (2011).
[44]N. R. Han, Z. C. Chen, C. S. Lim, B. Ng, and M. H. Hong, Opt. Express **19**, 6990–6998 (2011).
[45]K. Iwaszczuk, A. C. Strikwerda, K. Fan, X. Zhang, R. D. Averitt, and P. U. Jepsen, Opt. Express **20**, 635–643 (2012).
[46]A. P. Slobozhanyuk, M. Lapine, D. A. Powell, I. V. Shadrivov, Y. S. Kivshar, R. C. McPhedran, and P. A. Belov, Adv. Mater. **25**, 3409–3412 (2013).
[47]Y. J. Yoo, H. Y. Zheng, Y. J. Kim, J. Y. Rhee, J.-H. Kang, K. W. Kim, H. Cheong, Y. H. Kim, and Y. P. Lee, Appl. Phys. Lett. **105**, 041902 (2014).
[48]F. Zhang, Z. Liu, K. Qiu, W. Zhang, C. Wu, and S. Feng, Appl. Phys. Lett. **106**, 061906 (2015).
[49]B. Arritt, B. Adomanis, T. Khraishi, and D. Smith, Appl. Phys. Lett. **97**, 191907 (2010).
[50]X. Xu, B. Peng, D. Li, J. Zhang, L. M. Wong, Q. Zhang, S. Wang, and Q. Xiong, Nano Lett. **11**, 3232–3238 (2011).
[51]S. Lee, S. Kim, T.-T. Kim, Y. Kim, M. Choi, S. H. Lee, J.-Y. Kim, and B. Min, Adv. Mater. **24**, 3491–3497 (2012).
[52]Y. Cui, J. Zhou, V. A. Tamma, and W. Park, ACS Nano **6**, 2385–2393 (2012).
[53]J. Li, C. M. Shah, W. Withayachumnankul, B. S.-Y. Ung, A. Mitchell, S. Sriram, M. Bhaskaran, S. Chang, and D. Abbott, Appl. Phys. Lett. **102**, 121101 (2013).
[54]F. Zhang, S. Feng, K. Qiu, Z. Liu, Y. Fan, W. Zhang, Q. Zhao, and J. Zhou, Appl. Phys. Lett. **106**, 091907 (2015).
[55]A. K. Azad, J. Dai, and W. Zhang, Opt. Lett. **31**, 634–636 (2006).
[56]X. Lu, J. Han, and W. Zhang, Appl. Phys. Lett. **92**, 121103 (2008).
[57]The reference that is used for defining the reflection amplitude is the reflected signal taken from an aluminum-coated silicon wafer. It is worth noting that a total reflection mirror made of aluminum on 50-μm-thick Kapton film will be an ideal reference to get accurate reflection amplitude and phase shift. But in the actual measurement, the imperfect flatness of the 50-μm-thin Kapton film and its sensitivity to the surrounding disturbance will largely limit the performance of the THz-TDS setup. Furthermore, in the current work, we only focus on the reflection amplitude instead of the phase shift. The aluminum-coated silicon wafer has the advantage of being sufficient flat to provide a uniform reflection for the normalization process. Actually, we have adapted both the silicon and thin film reference in our measurements and found the aluminum-coated silicon had the better performance.

[58]P. K. Singh, S. Kabiri Ameri, L. Chao, M. N. Afsar, and S. Sonkusale, Prog. Electromagn. Res. **142**, 625–638 (2013).
[59]B. M. Fischer, M. Walther, and P. U. Jepsen, Phys. Med. Biol. **47**, 3807–3814 (2002).
[60]B. M. Fischer, M. Hoffmann, H. Helm, R. Wilk, F. Rutz, T. K. Ostmann, M. Koch, and P. U. Jepsen, Opt. Express **13**, 5205–5215 (2005).
[61]R. Mendis, V. Astley, J. Liu, and D. M. Mittleman, Appl. Phys. Lett. **95**, 171113 (2009).
[62]B. You, J. Y. Lu, C. P. Yu, T. A. Liu, and J. L. Peng, Opt. Express **20**, 5858–5866 (2012).
[63]W. Withayachumnankul, H. Lin, K. Serita, C. M. Shah, S. Sriram, M. Bhaskaran, M. Tonouchi, C. Fumeaux, and D. Abbott, Opt. Express **20**, 3345–3352 (2012).
[64]F. Fan, S. Chen, X. Wang, P. Wu, and S. Chang, IEEE Photon. Technol. Lett. **27**, 478–481 (2014).
[65]D. Wu, J. Liu, H. Han, Z. Han, and Z. Hong, Front. Optoelectron. **8**, 68–72 (2015).